

The Effect of Tip Angle on Cavitation Potential during Closure of a Bileaflet Prosthesis Model

Pei Zhang¹, Joon Hock Yeo², Ping Qian¹, Ned H. C. Hwang³

¹School of Mechanical & Automation Engineering, Shanghai Institute of Technology, China, ²School of Mechanical & Production Engineering, Nanyang Technological University, Singapore, ³Division of Medical Engineering, National Health Research Institute, Taiwan

Background and aim of the study: Mechanical heart valve (MHV) cavitation has been widely investigated by negative pressure transient (NPT) measurements. Whilst NPT is believed to be the cause of cavitation as the valve occluder approaches its fully closed position, some valves are also more prone to cavitation initiation. The study aim was to determine the effect of tip angle on the occluder trailing edge for the MHV closure flow field and cavitation potential.

Methods: Three pairs of 1:1 transparent bileaflet models, with different tip angles (30°, 60° and 90°), were used in a pulsatile mock loop. Particle image velocimetry (PIV) and micro-tip pressure catheters were applied respectively for the closure flow and transient pressure investigations. A mechanism was designed to enable triggering when the valve

occluder approached its closing position.

Results: The transient pressure showed two maximum pressure drops, the magnitudes of which differed with various angle designs. A series of flow fields with continuously narrowing gap channels was captured. Different flow features were demonstrated for the three valve models.

Conclusion: The tip angle design on the occluder trailing edge affected both the NPT magnitude and MHV closure flow field. The 60° and 30° valves had higher vorticity and fluid deceleration rate within the squeeze flow and occluder sudden stop respectively, which correlated with their larger pressure drops for the first and second NPT peaks.

The Journal of Heart Valve Disease 2007;16:430-439

Cavitation is the rapid formation and collapse of vaporous bubbles caused by a momentarily sharp local pressure drop below the vapor pressure (1). Some clinically explanted mechanical heart valves (MHVs) have been found to show erosions and pittings, which are typical signs of damage resulting from the collapse of cavitation bubbles (2). Both, the mechanism and origin of MHV cavitation are yet to be fully understood, although squeeze flow and water hammer are among two possible causes (3,4). As the valve occluder approaches its fully closed position, fluid which is 'trapped' between the occluder tip and the orifice wall has a tendency to be squeezed out, causing a high-speed jet flow. As the jet separates from the channel, it mixes instantaneously with the ambient liquid to form a strong shear layer that induces vortices. The cores of these vortices are low-pressure regions that can initiate cavitation. It is also believed that, the higher the vortex

intensity (i.e., vorticity) the lower the pressure produced (5), and this could explain the erosions observed along the valve circumferential edge (6). The water hammer effect normally refers to a pressure reduction at the upstream side upon valve closure. When the occluder comes to a sudden stop, the fluid proximal to the MHV surface will also stop. The fluid deceleration then causes the pressure to drop such that, the larger the deceleration rate the more the pressure is reduced (7).

Quantitative analyses performed by various investigators strongly suggest that MHV closing actions may cause transient, localized cavitation in the vicinity of the valve. Negative pressure transients (NPTs) on the ventricular side upon MHV closure were found to correlate with cavitation occurrence (8-10). MHV closure flow associated with the cavitation phenomenon was investigated both by experimental investigations (11-17) and computational fluid dynamics (CFD) studies (18-20).

From the aspect of fluid mechanics, the geometry of the approaching valve boundary would affect the MHV closure flow field and pressure distributions - that is, the potential occurrence of cavitation. Both,

Address for correspondence:

Qian Ping PhD, School of Mechanical & Automation Engineering, Shanghai Institute of Technology, 120 Cao Bao Road, Shanghai, China, 200235

e-mail: zhangpei7036@yahoo.com.cn/pg02232040@ntu.edu.sg

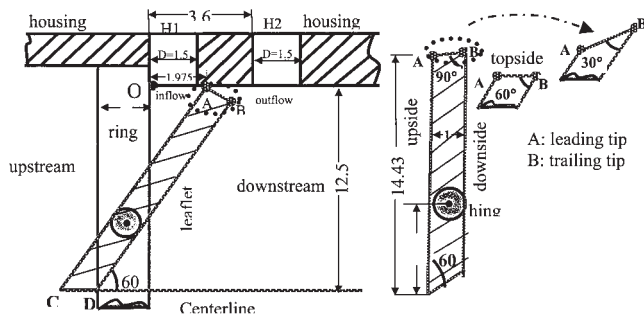


Figure 1: Schematic diagram of the 90° valve tip design upon full closure.

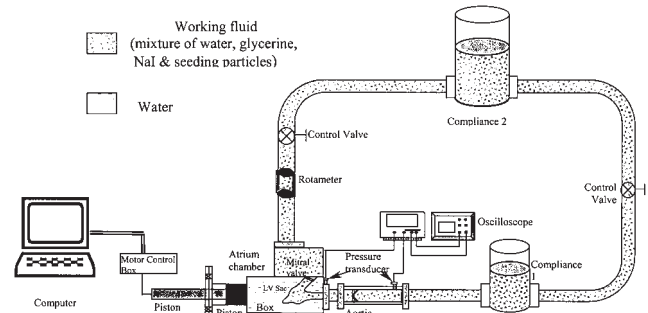


Figure 2: Schematic of the pulsatile flow test rig.

experimental and computational investigations in this regard have been carried out. When the closing dynamics of two impinging rods was used to study MHV cavitation with respect to squeeze flow, it was found that both the contact area and the magnitude of squeeze flow velocity influenced the onset and intensity of cavitation (16). Lee et al. (21), after studying nine different MHVs, believed that the occluder seat stop (a block mechanism on the housing wall, which would impact against MHV upon closure) was crucial to cavitation. A further investigation indicated that around the seat stop, bubbles were observed and pressures were found to fall below the liquid vapor pressure. It was therefore suggested that the fluid squeezing between the stop and the occluder was the main cause of cavitation (22). Numerical simulations have also shown that squeeze flow was mainly affected by the geometry of the gap channel, leaflet motion and valve mounting compliance (18,20).

Detailed studies associated with valve design factors, cavitation initiation and squeeze flow are still limited in number. In the present study, different geometries of the valve boundary were achieved by modifying the tip angle on the occluder trailing edge. Three sets of 1:1 MHV models with 30°, 60° and 90° angles were fabricated (see Fig. 1). Transient pressures occurring at different MHV models were recorded, together with flow velocity measurements upon valve closure, by using a particle image velocimetry (PIV) technique. In this way the relationship between the valve design, squeeze flow and the potential for cavitation can be correlated.

Materials and methods

Pulsatile flow test loop

The experimental set-up is illustrated in Figure 2. A computer-controlled servo-motor (SEM Controlled Motor Technology, UK) was used to drive an 8-cm diameter piston to produce pulsatile flow in the test loop. The motion curve of the piston could be created,

modified and implemented by a Programmable Transmission System (Quin Company, UK). An acrylic box, which connected with the piston head, was filled with water and accommodated a collapsible left ventricular sac. Upstream of the left ventricle, a left atrial chamber was connected with a commercial tilting-disk valve. An acrylic test section simulating the aorta was placed downstream of the left ventricle, and a transparent aortic valve model installed inside the test section. The afterload resistive and compliance elements placed downstream of the test section returned to the atrium, and could be tuned separately to obtain desirable physiologic pressures and flow rates. Two pressure transducers (Model T4812AD-R; Oxnard, CA, USA), coupled with a calibrated multi-channel amplifier (AM-PACK AP9991; Vivitro System), were used to measure the ventricular and aortic pressures immediately upstream of the aortic valve, and five aorta diameters downstream, respectively. The typical pressure waveforms recorded by an oscilloscope (Tektronix, TDS36) are shown in Figure 3; this was generally

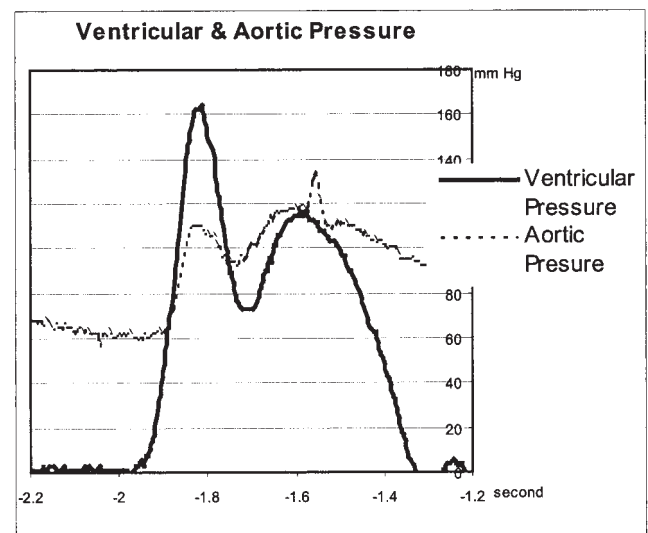


Figure 3: Typical ventricular and aortic pressure waveforms.

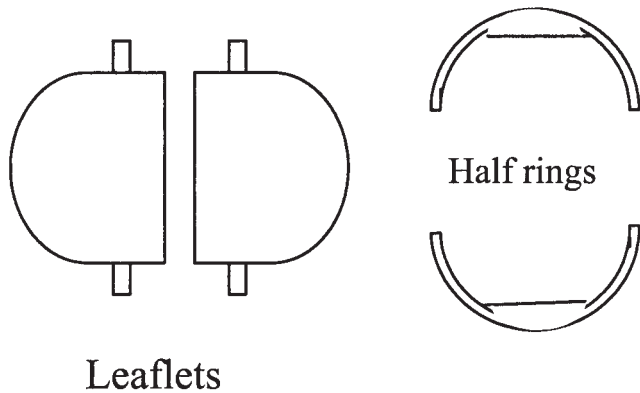


Figure 4: Schematic drawings of the mechanical heart valve model parts.

acceptable when referring to standard physiological pressures. The heartbeat was 63 per min with 40% systolic duration, and the mean flow rate 4.3 l/min. These parameters were set at the low limits of the physiological range in order to protect the transparent MHV model while under prolonged testing conditions. The ventricular and aortic pressures, as well as the flow rate, provided the physiological working conditions and were kept identical when the experiments for various MHV models were performed.

Transparent MHV model

The separate parts of an acrylic MHV model (see Fig. 4) were constructed using computer numerical controlling (CNC) machining. The transparency of the valve material enabled PIV measurements without obstruction. In order to approximately match those of a St. Jude Medical bileaflet valve, the length, radius and thickness of the parts were checked using a caliper, and the model's opening and closing angles were calculated from PIV images.

Three MHV models with different angles on the occluder trailing edge were fabricated (see Fig. 1); an image of a complete valve model is shown in Figure 5. The gap distance was defined as the width between the trailing tip and the housing wall.

Micro-tip pressure catheter

Two pressure measurement positions, H1 and H2 (as shown in Fig. 1), were drilled through the aortic wall, where pressure catheters of 1 mm diameter were positioned. The transient pressures were recorded simultaneously at both the ventricular and aortic sides. Measurements were made using two micro-tip pressure catheters (SPC-330A; Millar Instrument Inc., USA). The catheter had a natural frequency over 30 KHz, its pressure response ranged from 0 to approximately 10 KHz (33% of its natural frequency), and its overpressure ranged from -760 to 4,000 mmHg.

The pressure signal was amplified by a transducer control unit (Model PCB 500; Millar Instrument Inc.) and recorded using an AR1200 Analyzing Recorder (Yokogawa, Japan). The recorder was equipped with eight isolated analogue input channels and a 14-bit analogue/digital converter with a maximum sampling rate of 100 kS/s. The memory capacity was 64 K words per channel. The pressure signal was sampled at a rate of 20 KHz, and the data were transferred to a desktop computer for post-processing.

PIV system

A TSI Insight™ PIV system (TSI Inc., USA) was used in this study. The double-pulsed laser from two separate Nd:YAG systems (532 nm, maximum 50 mJ/pulse; MiniLase III, New Wave Research) provided illumination for the flow field plane. A CCD camera (1000×1016 pixel) was coupled with an X-Y traveling mechanism (0.01 mm adjustment step) and a Stemi 2000-C microscope (Zeiss) to precisely locate and observe the minute channel flow upon MHV closure. The displacement of particle images captured between two light pulses was determined through the evaluation of two PIV recordings by cross-correlation. With current PIV settings, the system spatial resolution was 90 μm and the size of the field of view approximately 2.7 mm.

When processing PIV images, a leaflet thickness of 1 mm was used to calibrate the velocity field. The corresponding vector files, created in Insight software, were loaded into Tecplot (Version 8.0, Tecplot, Inc., USA) to present the PIV data graphically.

Working fluid and seeding particles

The working fluid was composed of 79% saturated aqueous sodium iodide, 20% pure glycerol and 1% distilled water, by volume. This composition yields a

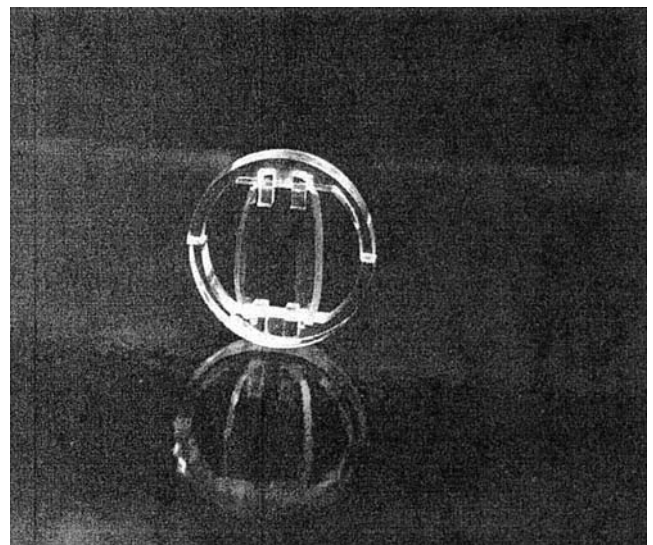


Figure 5: The transparent mechanical heart valve model.

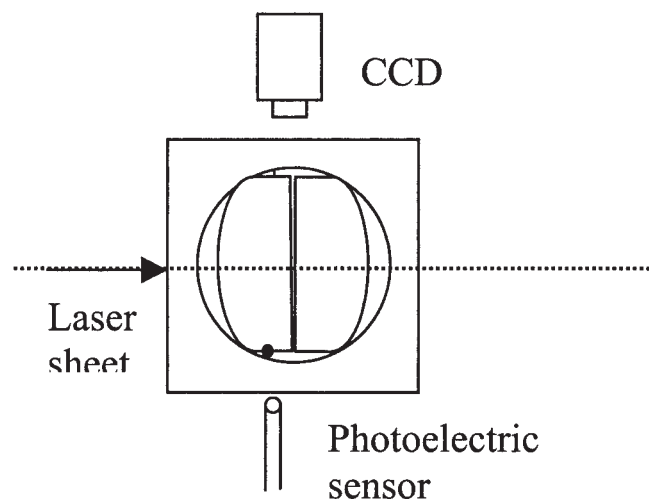


Figure 6: Diagram illustrating the position of the photoelectric sensor (cross-section of the mechanical heart valve). CCD: Charge-coupled device camera.

kinematics viscosity of 3.4 cS, matching that of human blood at high shear rates. The refractive index of this fluid was measured as 1.49, the same as that of the acrylic test section, hence eliminating refractive deformation from the light passing through the curved liquid-solid interface. The seeding particles, which were 10 μm silver-coated glass spheres, were selected due to their good image contrast and suitable particle image diameter.

Triggering set-up

The frame rate of the charge-coupled device (CCD) camera was 30 per second, which was grossly insufficient for analyzing the MHV closing process of less than 50 ms. Hence, a triggering method was developed. A photoelectric sensor (HPX-NT1, Yamatake Japan; see Fig. 6) captured the closing movement of the MHV leaflet. The sensor signal was input to an Intel 82C54 Programmable Interval Counter/Timer (1600 Data Acquisition Board, Keithley Instruments), which produced a time delay in the signal. The triggering instant was selected immediately before the valve was fully closed, and may have differed for the three different occluder designs due to relocation of the photo-

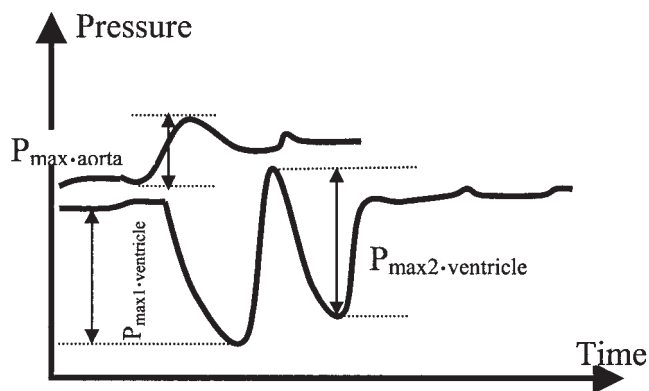


Figure 7: Graphical representation of the transient pressure drop and rise.

electric sensor when replacing the valve models. The signal with a 10 μs delay step was connected with a synchronizer for triggering data acquisition by PIV. Two consecutive PIV images were captured in one cardiac cycle. A total of 100 cycles of images was saved, from which those with the occluder in a specific position were selected for post-processing.

Results

Transient pressure

For the purpose of comparison, two transient parameters $P_{\text{max1.ventricle}}$ and $P_{\text{max2.ventricle}}$ were selected, which were the relative pressure drops for the first and second NPT peaks on the ventricular side. $P_{\text{max.aorta}}$ was the maximum pressure rise relative to the aortic pressure (see Fig. 7). Typical pressure waveforms for the angles of 30°, 60° and 90° were recorded (see Fig. 8a-c). The transient pressures at both the ventricular and aortic sides were found to experience dramatic changes upon MHV closure. The mean values of $P_{\text{max1.ventricle}}$, $P_{\text{max2.ventricle}}$ and $P_{\text{max.aorta}}$ over 50 cycles are summarized in Table I.

Among the three different angles on the valve trailing edge, the maximum pressure drop for the first NPT peak (i.e., $P_{\text{max1.ventricle}}$) was observed with the 60° valve, while 30° MHV created the largest magnitude of $P_{\text{max2.ventricle}}$ and the lowest $P_{\text{max1.ventricle}}$ value. For the 60°

Table I: Average pressure rise and drop at different tip angles.

Valve tip angle (°)	Ventricular side		Aortic side	
	$P_{\text{max1.ventricle}}$ (mmHg)	$P_{\text{max2.ventricle}}$ (mmHg)	$P_{\text{max2.ventricle}}$ (mmHg)	$P_{\text{max.aorta}}$ (mmHg)
30	-253	-320	-320	94
60	-312	-183	-183	91
90	-283	-151	-151	104

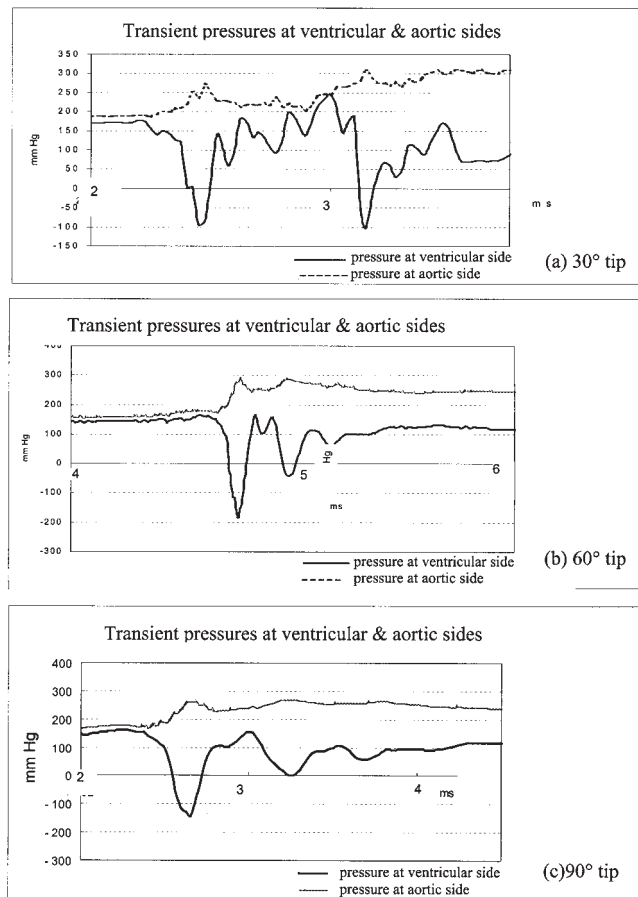


Figure 8: Transient pressures at the ventricular and aortic sides for different valve tip designs.

and 90° designs, $P_{\max 2, \text{ventricle}}$ was 40 to 55% lower than that of the 30° occluder. The outflow pressure rises for the 30° and 60° valve models were of similar magnitude, and the pressure rise for the occluder with 90° angle was marginal.

MHV tip velocity

The MHV average tip velocity within Δt , was calculated by analyzing the leaflet positions in PIV images (Δt was the duration between the zero instant and the leaflet full-closure instant). By fine-tuning the sensor

position, the zero instant could be chosen from different positions in the MHV closing process. With the magnification increasing, the zero instant was selected gradually closer to the leaflet full-closure position. Thus, the leaflet tip velocities within the decreasing gap dimensions were obtained (see Table II). It could be shown, that the MHV tip velocity was increasing as the occluder gradually approached the orifice wall, with a magnitude of 0.24 m/s in the final 10° of the valve closure journey.

Closure flow field

Case A: Gap ca. 0.5 mm

The flow velocity maps for various valve tips when the gap width was approximately 0.5 mm are shown in Figure 9. The three types of occluder had similar velocity magnitudes both in the upstream and downstream regions, with maximum values between 0.76 and 0.81 m/s. Some similar flow features, such as the downstream flow perpendicular to the leaflet surface and the upstream flow parallel to the axial direction, were observed for the three valve designs.

Case B: Gap ca. 0.1 mm

As the gap dimension was decreased, fluid momentum increased both upstream and downstream. When the gap decreased to approximately 0.1 mm, a high-speed squeezing jet was observed outside the gap for the 60° and 90° valve tips (see Fig. 10b and c). The 60° design had the largest squeezing velocity (ca. 2.1 m/s) at the exit of the gap, and also demonstrated a higher vorticity around its leading tip, with a magnitude up to 2,200 per second.

For the 30° valve tip, the squeeze flow phenomenon was difficult to observe. Although its map (see Fig. 10a) had a gap dimension less than 0.1 mm, the flow speed at the gap exit did not have a much higher magnitude than the nearby regions, resulting in a relatively low vorticity of approximately 1,200 per second. Its flow structure actually inherited the characteristics at larger gap dimensions.

Case C: Occluder sudden stop

Immediately after squeeze flow, the occluder came to

Table II: Average leaflet velocity within various gap dimensions.

Magnification	α at:		Δt (ms) tip velocity	Average leaflet (m/s)
	$t = 0$ ms	full closure		
0.28	72°	30°	55	0.14
1.8	63°	30°	35	0.16
3.2	40°	30°	6.5	0.24

α = angle between leaflet and transverse direction.

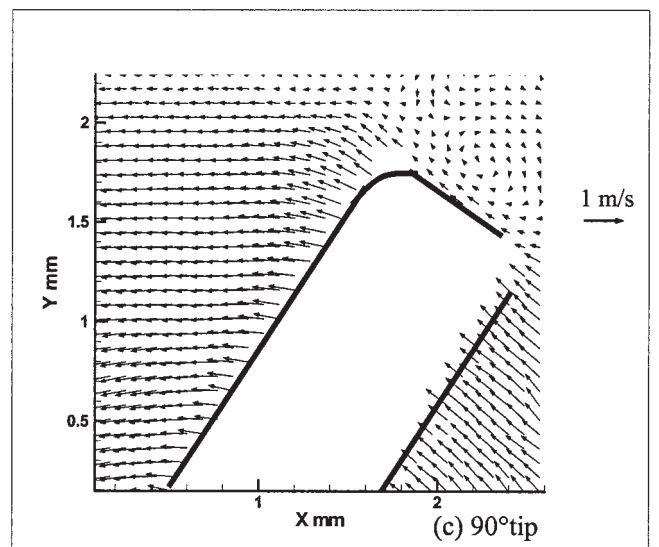
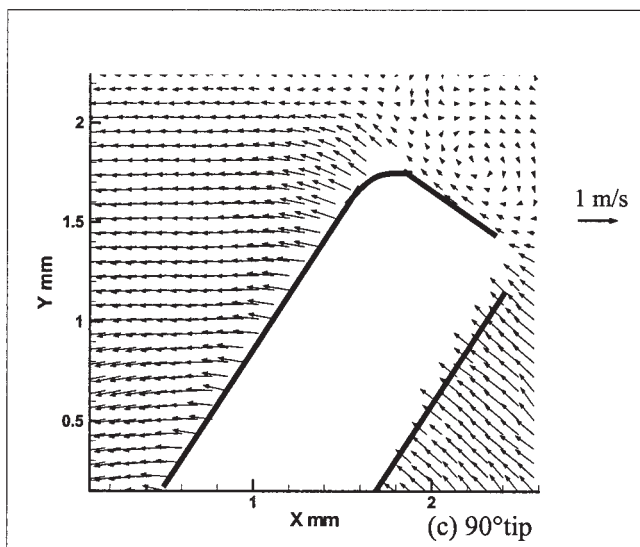
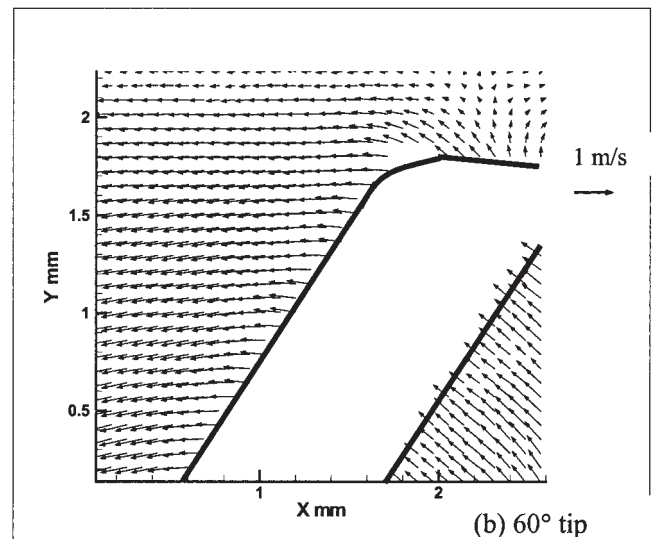
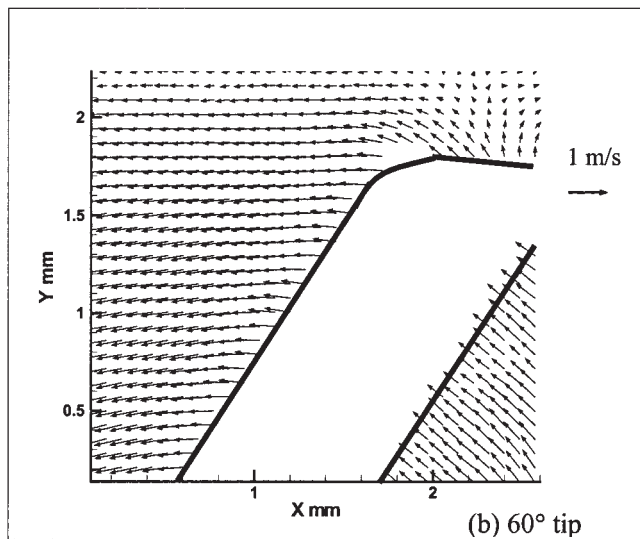
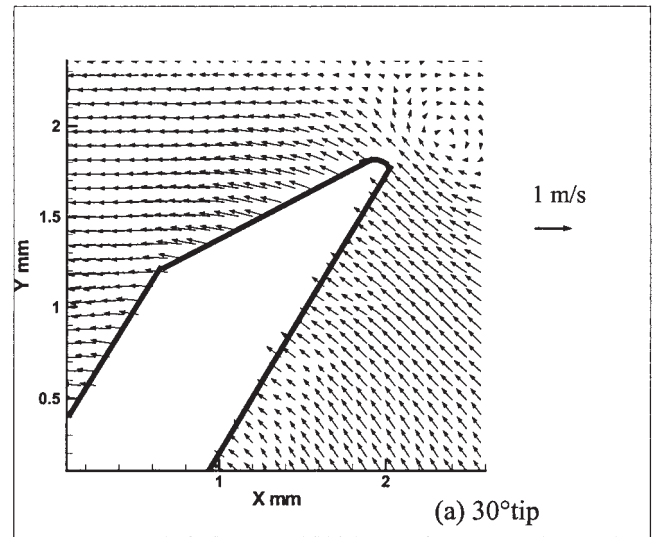
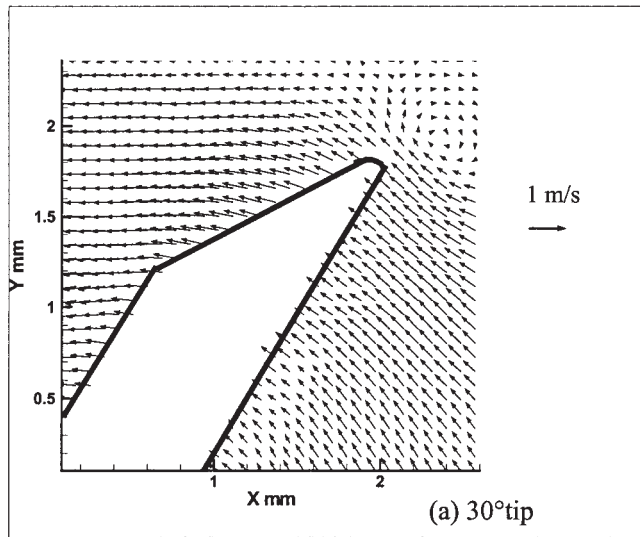


Figure 9: Velocity maps when the gap is approximately 0.5 mm.

Figure 10: Velocity maps when the gap is approximately 0.1 mm.

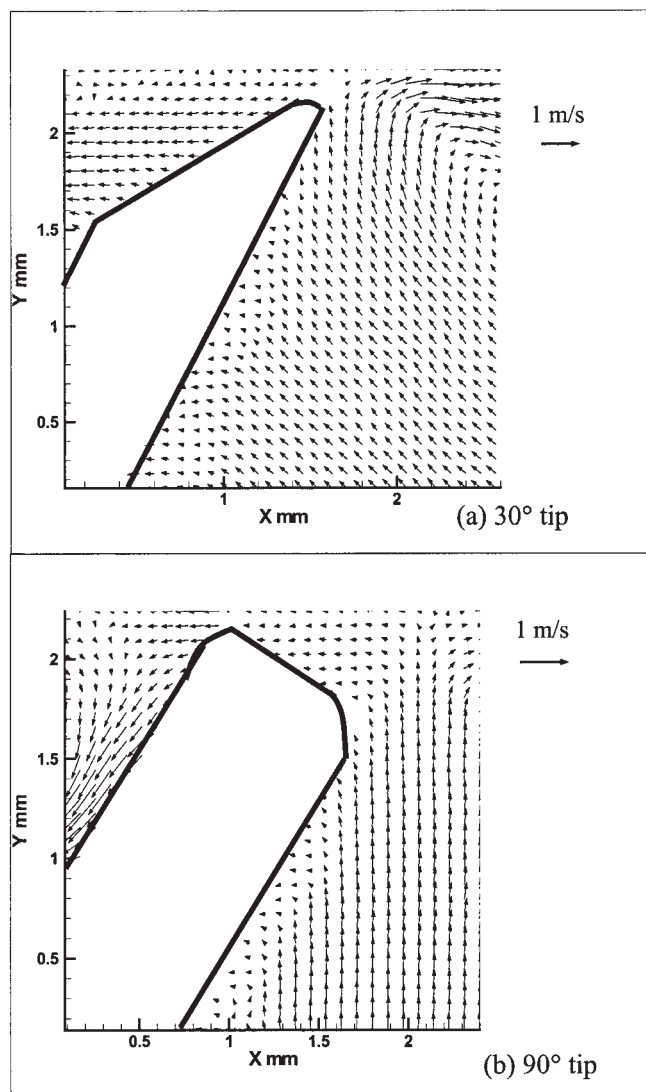


Figure 11: Velocity maps upon occluder sudden stop.

a sudden stop (see Fig. 11). Although the occluder was still pushed by the backflow, the driving action was dramatically reduced, with velocities between 0 and 0.15 m/s. The flow on the ventricular side was also sharply decreased in magnitude due to the dramatically reduced momentum transferred from the occluder upon its sudden stop. The 90° valve tip was found to have a relative higher flow velocity than other designs during this period.

Discussion

Cavitation in the aortic position

The main object of the present study was to determine the effect of occluder tip design on MHV closure flow and cavitation potential. Although the mitral valve is more prone to cavitation initiation, the aortic

position was finally selected in these investigations due to the difficulty of carrying out PIV experiments in the mitral position and based on the compromised considerations of the current test rig arrangement. The cavitation potential, however, was indicated by the magnitude of local pressure drop.

The results showed that the three different valve designs had a maximum NPT at approximately -300 mmHg on the ventricular side. This condition would not initiate cavitation as the pressure was not as low as the fluid vapor pressure (-740 mmHg at 25°C for water). However, in the mitral position, where the valve closing pressure was expected to be greater, a lower NPT was produced which, in some extreme cases, was sufficiently low as to induce cavitation.

Effects of tip angle on the closure flow field

Various MHV models demonstrated some similar features for the pre-squeeze flow field. When the gap distance was approximately 0.5 mm, the downstream flow was perpendicular to the leaflet surface, which may have been the cause of the MHV closure motion. The upstream flow was parallel to the axial direction, possibly as a result of the combined effects of the momentum transfer from the occluder's displacement, squeeze flow from the gap, and the occluder translation movement. The occluder translation was due to the hinge clearance, which was necessary for free rotation. During this pre-squeeze flow phase, the influences of different tip geometries were demonstrated by the position where the wake was formed around the leaflet: The sharper the occluder tip, the later the vortex emerged along the leaflet edge.

The 30° and 90° valve tips were found to be less prone to squeeze flow than the 60° valve tip. Due to their sharp tip geometries, the gap structures played only a minor role in speeding up the backflow inside the gap, and this may be the reason for their relative low magnitudes of squeeze flow velocities. The 60° valve tip however, had a larger squeeze flow velocity at the immediate exit of the gap (possibly resulting from the narrower gap width) than the other designs. When the squeezing jet had exited the gap it mingled with a low-momentum flow region, forming a strong vorticity in this region.

During the occluder sudden stop, the 30° occluder featured a relatively lower flow velocity on the ventricular side compared to the 90° occluder. One possible explanation for this is that the wider gap structure of the 90° occluder still enabled a weak backflow to the ventricular side through the gap. If the duration of the flow velocity change upon MHV stopping was assumed identical for various valve designs, the 30° occluder was considered to have a higher flow deceleration rate at the ventricular side. Thus, a large pres-

sure drop may be initiated for this valve model.

Relationships between NPT, closure flow, and tip angle

Squeeze flow and occluder sudden stop are, therefore, suggested to produce local pressure drops for potential cavitation. It is hypothesized that NPT peaks shown on the ventricular side are due to the squeeze flow, water hammer effect and/or possible occluder rebound. From a temporal domain, the first NPT peak is possibly related to the squeeze flow phenomenon, while the second NPT peak may be associated with a different effect - that is, the water hammer effect and a possible rebound motion. When the squeeze flow occurred at the gap exit, the 60° tip design created the highest vorticity of approximately 2,200 per second, which was almost twice that seen for the 30° valve. This may correlate respectively with the largest and lowest magnitudes of the first NPT peaks of the two valves, at about -310 mmHg and -250 mmHg. Compared to the 90° valve, the 30° tip design had a more evident fluid deceleration rate upon stopping, which induced its relatively large transient pressure of -320 mmHg during the second NPT peak.

Hence, for the future development of MHV prostheses, the influences of the geometries of the MHV trailing edge on cavitation potential should be taken into account. Different tip angles result in different gap structures in the final journey of the MHV closing process, which in turn affects both the closure flow field and local pressure drop. It was found that, the wider the gap dimension upon squeeze flow and occluder sudden stop, the less possible cavitation would occur. However, from a clinical perspective, a relatively large gap width would cause valve incompetence. Hence, the ideal design may be a compromise between these two aspects.

Comparisons with previous studies

Occluder tip velocity

Factors affecting MHV cavitation and associated flow characteristics have been studied extensively during the past decade. MHV occluder closure behavior is believed to be the key factor in MHV cavitation, which has a strong correlation with the valve type, heart rate, and cardiac output (4,8,11,12). By using a laser sweeping technique (LST), the tip velocity of a mitral pyrolytic carbon (PyC) valve was found to be in the range of 0.52 ± 0.15 to 1.64 ± 0.38 m/s within its last 3° of closure journey (12). However, in the present study, the analysis of PIV images showed that the aortic MHV model had a closure velocity of approximately 0.24 m/s during the final 10° of the closing process. This relatively low closing velocity could be attributed to the varied time intervals of the measurements, as

the occluder velocity was increasing during the closing process. Second, the aortic valve, when compared to the mitral valve, had a lower rate of pressure change upon closure (dp/dt). Additionally, the valve closure behavior was not simulated physiologically in these studies due to a lack of control over dp/dt and density differences between acrylic and PyC.

Although studies of valve-closing motion using the PIV approach lack the high resolution of LST, the procedure is both rapid and convenient, and also allows simultaneous observation of the flow field.

Squeeze flow

The transient and complicated MHV closure flow field, including squeeze flow, sudden stop and/or possible rebound - all of which occur within the order of a few microseconds - raises challenging tasks for both experimental and CFD studies. Although the transparent MHV model facilitates fluid observation between the occluder edge and housing wall, the current PIV system is still limited in the squeeze flow study with gaps of approximately 100 μ m in width. In theory, the PIV spatial resolution of 90 μ m can produce one velocity vector in an interrogation area of 90 \times 90 μ m, but in practice - due to the particle specifications and in-plane and out-of-plane losses of image pairs - it is difficult to guarantee that the micron gap is densely seeded, which is essential for correct measurement. Hence, many PIV pictures are required to study this phenomenon. In the present study, very little information was provided regarding the velocity distributions inside the gap channel. Rather, at the immediate exit of the channel a relatively wide region was created by the curvature of the occluder tip (due to the manufacturing process), where a large squeeze velocity and also a strong vorticity were found. Maymir et al. (13) also reported similar squeeze flow velocities, with magnitudes of 1.67 m/s in the aortic position and 3.02 m/s in the mitral position of a monostrut valve by using laser Doppler anemometry (LDA, sample volume of 140 \times 20 μ m). Kini et al. (14) used both PIV and LDA methods to investigate the flow downstream of a Björk-Shiley valve in the mitral position. The LDA results provided the fine temporal variation of fluid dynamics associated with occluder first closure and rebound, while PIV proved to be more intrusively quantitative in the two-dimensional flow map. The fluid velocities were found to be between 2.0 and 2.5 m/s at closure and rebound instants. Chandran et al. (15) reported an approximate estimation of squeeze flow velocity of 12 m/s in a flow loop simulating a single closing event of the mitral valve. The cavitation bubbles were imaged and the squeeze flow velocity was calculated from the distance between similar bubbles, assuming that these had been caused by squeeze flow and that the same bubble's

radial motion was followed.

Current mathematical models of the MHV closing process suffer from problems in simulating unsteady flow, moving boundaries, turbulence, and solid-fluid interactions. However, by simplifying some of these factors, Bluestein et al. (18) estimated that a squeeze velocity above 14 m/s would cause cavitation; that is, a local pressure below -760 mmHg based on the Bernoulli principle. With a constant leaflet tip velocity of 4m/s as the input, numerical simulations showed that Edward-Duromedics mitral valves had a squeeze flow velocity of up to 30 m/s in the gap space when the gap dimension was in the order of micrometers (18). When applying the experimentally measured curve of the occluder closing velocity, and also considering leaflet deceleration and rebound, a relatively low squeeze flow velocity was calculated at approximately 9 m/s (19).

In conclusion, the tip angle design on the occluder trailing edge was found to affect both the NPT magnitude and the closure flow field. The 60° valve demonstrated higher magnitudes of squeeze flow velocity and vorticity when the gap was approximately 0.1 mm, while the 30° model had a lower flow velocity and a larger deceleration rate upon occluder sudden stop. The larger magnitudes of vorticity and fluid deceleration occurring with these two MHV designs correlated respectively with their larger pressure drops for the first and second NPT peaks. It is suggested, therefore, that a relatively wide gap dimension would be prone to reducing the squeeze vorticity and the subsequent fluid deceleration rate, and hence minimize the possibility of cavitation initiation.

Acknowledgements

These studies were supported by the Shanghai Science and Technology Committee, Project No. 06PJ14083, and the School of Mechanical and Aerospace Engineering in Nanyang Technological University (NTU), Singapore.

References

1. Young FR (ed.), Cavitation. McGraw-Hill, London, 1989
2. Klepetko W, Moritz A. Leaflet fracture in Edwards Duromedics bileaflet valves. J Thorac Cardiovasc Surg 1989;97:90-94
3. Hwang NHC. Cavitation potential of pyrolytic carbon heart valve prostheses: A review and current status. J Heart Valve Dis 1998;7:140-150
4. Wu ZJ, Wang Y, Hwang NHC. Occluder closing behavior: A key factor in mechanical heart valve cavitation. J Heart Valve Dis 1994;3(Suppl.I):S25-S34

5. Rood EP. Review: Mechanisms of cavitation inception. J Fluids Eng 1991;113:163-175
6. He ZM, Xi BS, Zhu KQ, Hwang NHC. Mechanisms of mechanical heart valve cavitation: Investigation using a tilting disk valve model. J Heart Valve Dis 2001;10:666-674
7. Freed D, Walker WF, Dube CM, Tokuno T. Effects of vaporous cavitation near prosthetic surfaces. Am Soc Artif Intern Organs Trans 1981;27:105-109
8. Chandran KB, Lee CS, Chen LD. Pressure field in the vicinity of mechanical valve occluders at the instant of valve closure: Correlation with cavitation initiation. J Heart Valve Dis 1994;3(Suppl.I):S65-S76
9. Garrison LA, Lamson TC, Deutsch S, Geselowitz DB, Gaumond RP, Tarbell JM. An in vitro investigation of prosthetic heart valve cavitation in blood. J Heart Valve Dis 1994;3(Suppl.I):S8-S24
10. Chandran KB, Dexter EU, Aluri S, Richenbacher WE. Negative pressure transients with mechanical heart valve closure: Correlation between in vitro and in vivo results. Ann Biomed Eng 1998;26:546-556
11. Wu ZJ, Gao BZ, Hwang NHC. Transient pressure at closing of a monoleaflet mechanical heart valve prosthesis: Mounting compliance effect. J Heart Valve Dis 1995;4:553-567
12. Wu ZJ, Hwang NHC. Asynchronous closure and leaflet impact velocity of bileaflet mechanical heart valve. J Heart Valve Dis 1995;4(Suppl.I):S38-S49
13. Maymir JC, Deutsch S, Meyer RS, Geselowitz DB, Tarbell JM. Mean velocity and Reynolds stress measurements in the regurgitant jets of tilting disk heart valves in an artificial heart environment. Ann Biomed Eng 1998;26:146-156
14. Kini V, Bachmann CF, Deutsch AS, Tarbell JM. Integrating particle image velocimetry and laser Doppler velocimetry measurements of the regurgitant flow field past mechanical heart valves. Artif Organs 2001;25:136-145
15. Chandran KB, Chew YT, Low HT, Lim WL, Seng KY. In vitro demonstration of squeeze flow at the instant of mechanical heart valve closure. ASME Adv Bioeng 1998;39:75-76
16. Lim WL, Chew YT, Low HT, Foo WL. Cavitation phenomenon in mechanical heart valves: The role of squeeze flow velocity and contact area on cavitation initiation between two impinging rods. J Biomech 2003;36:1269-1280
17. Manning KB, Kini V, Fontaine AA, Deutsch S, Tarbell JM. Regurgitant flow field characteristics of the St. Jude bileaflet mechanical heart valve under physiologic pulsatile flow using particle image velocimetry. Artif Organs 2003;27:840-846
18. Bluestein D, Einav S, Hwang NHC. A squeeze flow phenomenon at closing of a bileaflet mechanical

- heart valve prosthesis. *J Biomech* 1994;27:1369-1378
19. Makhijani VB, Yang HQ, Singhal AK, Hwang NHC. An experimental-computational analysis of MHV cavitation: Effect of leaflet squeezing and rebound. *J Heart Valve Dis* 1994;3(Suppl.I):S35-S48
 20. Makhijani VB, Siegel JM, Hwang NHC. Numerical study of squeeze-flow in tilting disc mechanical heart valves. *J Heart Valve Dis* 1996;5:97-103
 21. Lee CS, Chandran KB, Chen LD. Cavitation dynamics of mechanical heart valve prostheses. *Artif Organs* 1994;18:138-142
 22. Lee CS, Chandran KB, Chen LD. Cavitation dynamics of Medtronic Hall mechanical heart valve prosthesis: Fluid squeezing effect. *J Biomech Eng* 1996;118:97-105
 23. Lee CS, Aluri S, Chandran KB. Effect of valve holder flexibility on cavitation initiation with mechanical heart valve prostheses: An in vitro study. *J Heart Valve Dis* 1996;5:104-113
 24. Shi YB. Numerical and experimental study of pulsatile flow in bileaflet mechanical heart valves. Nanyang Technological University, Singapore, PhD thesis, 1998
 25. Adrian RJ. Particle-imaging techniques for experimental fluid mechanics. *Annu Rev Fluid Mech* 1991;23:261-304
 26. Brucker C, Steinseifer U, Schroder W, Reul H. Unsteady flow through a new mechanical heart valve prosthesis analyzed by digital particle image velocimetry. *Meas Sci Tech* 2002;13:1043-1049
 27. Chandran KB, Aluri S. Mechanical valve closing dynamics: Relationship between velocity of closing, pressure transients, and cavitation initiation. *Ann Biomed Eng* 1997;25:926-938
 28. Ellis JT, Healy TM, Fontaine AA, Weston MW. An in-vitro investigation of the retrograde flow fields of two bileaflet mechanical heart valves. *J Heart Valve Dis* 1996;5:600-606
 29. Maymir JC, Deutsch S, Meyer RS, Geselowitz DB, Tarbell JM. Effects of tilting disk heart valve gap width on regurgitant flow through an artificial heart mitral valve. *Artif Organs* 1997;21:1014-1025
 30. Prasad AK, Adrian RJ, Landreth CC, Offutt PW. Effect of resolution on the speed and accuracy of particle image velocimetry interrogation. *Exp In Fluids* 1992;13:105-116
 31. Subramanian A, Mu H, Kadambi JR, Wernet MP, Brendzel AM, Harasaki H. Particle image velocity investigation of intravalvular flow fields of a bileaflet mechanical heart valve in a pulsatile flow. *J Heart Valve Dis* 2000;9:721-731